Influence of water on the structure of anion deficient perovskite $BaSr_2TaO_{5.5}$

Labib. A. Awin[1*], Brendan.J. Kennedy[2] and Abduladhim Ali Alarabi[3]

[1]Chemistry Department, Faculty of Science, Tripoli University, Libya
[2]School of Chemistry, The University of Sydney, Sydney, NSW 2006 Australia
[3]Material science Department, Higher Institute of Sciences and Technology, Gharyan. Libya.

L.Awin@uot.edu.ly.

الملخص

في هدا العمل تم اختبار طريقة جديدة لاصطناع فراغات أكسجينية في تركيب البيروفسكايت. الطرق المدروسة كانت علي أساس تفاعلات الحالة الصلبة ولكن باستخدام اوساط طينية مختلفة محددة من الاسيتون والماء. الغرض من هذ *الاوساط* هو تحسين من تجانس المخاليط ، وأيضاً لخلق وسط جاف ورطب للتفاعل الأولي. الهدف الرئيسي لهده الدراسة هو فحص تأثير الوسط الطيني المائي علي الخصائص التركيبية للبيروفسكايت $BaSr_2TaO_{5.5}$.هذا وتم تشخيص الأكسيد بواسطة: المجهر الإلكتروني، جهاز التحليل الوزني الحراري، جهاز حيود الأشعة السينية وحيود النيترونات.

المركب المحضر له تركيب بلوري من نوع المكعب ممركز الأوجه مع مجموعة فراغية $Fm\bar{3}m$. كلا طريقتي التحضير انتجتا مساحيق أحادية الطور لكنها تختلف في اللون، حجم الحبيبات، والصلابة. حجم وحدة الخلية لبلورة الاكسيد المتحصل عليه من خلط المتفاعلات مع الماء كانت اكبر من تلك المتحصل عليها بواسطة خلط الخليط مع الاسيتون. نتائج منحنيات الحيود النيتروني اوضحت أن الكاتيونات وأيونات الأكسجين كانت غير منتظمة في التركيب. التمدد الحراري غير العادي لوحدة الخلية كان بسبب وجود الماء وخلل الانيون داخل التركيب.

Abstract

In the present work, a new method for creating oxygen vacancies in the perovskites structure was investigated. The methods studied were based on solid-state reactions but used different slurry medium, namely acetone and water. The purpose of the solvents is to enhance the homogeneity of the mixtures, and to create dry and wet media for the initial reaction. The main aim of the study is to investigate the impact of an aqueous slurry medium on the structural characteristics of the $BaSr_2TaO_{5.5}$ perovskite. The oxide was characterized by scanning electron microscopy, thermogravimetric analysis, and X-ray and neutron diffraction. The compound was prepared and has a face centered cubic structure with space group $Fm\bar{3}m$. The two synthetic methods produce monophasic powders and these differ in color, particle size, and hardness. The cell edges of the oxides obtained by mixing the reactants with water are larger than these obtained when the mixing was conducted with acetone. The neutron diffraction profiles

demonstrate that *A* cation and oxygen ions are disordered in the structure. The unusual thermal expansion of the unit cell is due to the presences of water and anion deficiency into the oxides structures.
Key words: perovskite structure, Influence of water.

Introduction

The structure of the ordered defect *double* perovskites of the type $A_2B^*BO_{5.5}$ where *A* and B^* = Ca^{2+}, Sr^{2+} or Ba^{2+} and *B* = Ta^{5+} are of current interest, since the mechanism of water interaction and the proton diffusion in the structure are critical in determining the electrical properties of such systems [1,2]. The title double perovskites exhibit ionic conductivity [3] and can absorb significant amounts of water to become proton conductors [4,5]. Unlike stoichiometric ABO_3 perovskites, in which all the *B*- type cations are six coordinate, the effective coordination number of the cations in anion-deficient $A_2B^*BO_{5.5}$ perovskites is reduced from six, so that locally some *B*- type cations will be five, or even four, coordinate [6]. Water can be incorporated into the lattice by occupying either the vacancies or nearby interstitial sites. The site which the incorporated water occupies will be dependent on the differences in the coordination tendencies of the B^* and *B* cations [6].

The typical crystal chemical effects observed in the $A_2B^*BO_{5.5}$ oxides include *B*-cation ordering [7] and/or structural distortions approximated by rotation of the nearly rigid BO_6 octahedra [8]; both effects are known to substantially influence the properties of these oxides [7,9]. A common approach to tune the structure of perovskites is substitution of the cation at the octahedral site forming oxides of the type, $AB_{1-x}B^*_xO_3$. In situations where $x \sim 0.5$ and when the size and/or charge of these two cations are sufficiently different the materials exhibit a 1:1 ordering of the two *B*-site cations, with alternating layers of the BO_6 and B^*O_6 octahedra along the [111] axis of the cubic cell, leading to a doubling of the unit cell lattice parameter [10,11]. The *A* site cations occupy every void that exist between 4 BO_6 and 4 B^*O_6 octahedra resulting in a three-dimensional arrangement that has the same topology as that of the anions and cations in the rock-salt structure [11,12]. In the non-stoichiometric $A_2B^*BO_{5.5}$ oxides, *B*-site ordering has been reported where the two nominally octahedrally coordinated cations display a rock salt like ordering [13,14,15].

Recently, the average and local crystal structures of the perovskites $Sr_2MSbO_{5.5}$ (*M* = Ca^{2+}, Sr^{2+} and Ba^{2+}) have been reported [15,16]. These adopt a faced centered cubic double perovskite structure with space group $Fm\bar{3}m$ and exhibit 1:1 cation ordering. An unusual feature of these oxides is the presence of a displacive

disorder of both the *A* site cations and oxygen anions [15]. In addition these oxides display anomalous thermal expansion of the lattice parameters as a consequence of local clustering of the vacancies and/or the anions with absorbed water molecules [15]. Studies of the local structure using pair distribution function (PDF) analysis of the neutron diffraction data showed that the SbO_x polyhedra adopt distorted trigonal bipyramids as a consequence of movement of oxygen into interstitial positions. This increases the coordination number of the *B* site cation from 5 or 6, to 6 or 7, and decrease the *A* site coordination number from 12 to 11. It is postulated that the movement of the oxygen into the interstitial sites is coupled with large displacements of the *A* and *B* site cations and, for $M = Sr^{2+}$, 45º rotations of the SbO_x polyhedra [16]. The two previous neutron diffraction studies provided no evidence for long range ordering of the oxygen vacancies in the structure but clearly a considerable amount of short range ordering does exist.

Experimental Work

The preparation of samples involved different stoichiometric compositions of Ta_2O_5 (Aldrich, 99.99 %) and $SrCO_3$ or $BaCO_3$ (Aithaca, 99.98 - 99.99 %). The mixtures were initially ground, as either an acetone or aqueous slurry, and preheated at 850 °C for 12 h, and then reground and heated at 1100 °C for 48 h. The crystallography of the samples was monitored by X-ray powder diffraction. Variable temperature powder X-ray diffraction data were collected on a PANalytical X'Pert X-ray diffractometer using Cu Kα radiation and a PIXcel solid-state detector.

Room temperature synchrotron X-ray powder diffraction data were collected over the angular range $5 < 2\theta < 85°$, using X-rays of wavelength 0.82518 Å on the powder diffractometer at the Australian Synchrotron [17]. For these measurements each sample was housed in a 0.3 mm diameter capillary. The structures were refined using the program RIETICA [18]. The peak shapes were modelled using a pseudo Voigt function. Neutron powder diffraction data were measured at 293 K using the high resolution powder diffractometer, Echidna [19], at the OPAL facility (Australian Nuclear Science and Technology Organization) at a wavelength of 1.6220 Å.

Thermal gravimetric analysis was conducted using a TGA 2950. The data were recorded under atmosphere of pure N_2 in order to examine weight loss under inert condition. Samples were analyzed up to a maximum temperature of 800 °C using a heating rate of 10 °C per minute and purge rate of between 40 and 60 mL/min. The microstructure of the powder samples was examined by scanning electron microscopy using a Intellection Quemscan**.**

Results and discussions:

Visually, it was observed that the colour of the powdered compound obtained using either acetone or water during the mixing is slightly different. The powder of $BaSr_2TaO_{5.5}$ is dark yellow when prepared using acetone whereas it is light yellow if water is used in the initial mixing. The hardness of the powders was found to be dissimilar; generally samples are much smoother after mixing with water. SEM analysis also revealed that the particle sizes were not equal. These surprising observations indicate that the presence of water in the initial stage of the reaction leads to larger crystallites and this is probably the basis for the differences in appearance and texture. Figure 1 demonstrates, as an example, SEM images for $BaSr_2TaO_{5.5}$. The grains are monophasic and apparently free of impurities, as confirmed by EDX analysis. The quantitative element analysis indicated that a chemical composition is consistent with the expected stoichiometry.

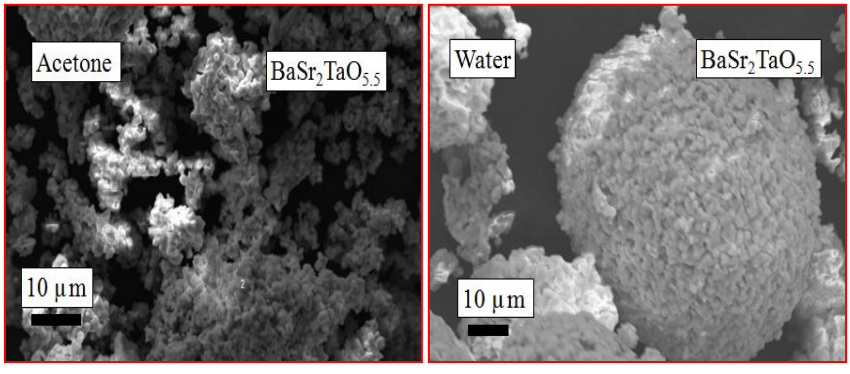

Figure 1: Scanning Electron Micrograph images for $BaSr_2TaO_{5.5}$ obtained using either acetone or water during the mixing.

Crystal Structure

The synchrotron X-ray powder diffraction patterns of the oxide exhibited strong (111) reflections indicative of 1:1 ordering of the *B*-site cations. No splitting or asymmetry of the cubic reflections was detected in the diffraction patterns indicating the structure was cubic, and the appropriate space group was $Fm\bar{3}m$. The materials can be formulated as $(BaSr)SrTaO_{5.5}$ in order to emphasize the ordering at the *B* site between the Sr and, Ta) cation. In the double perovskite structure, it is anticipated that the two smallest cations will order in the octahedral sites, this ordering being a consequence of the differences in the size and/or charge between the two cations [27]. The largest cation will then occupy the 12-coordinate

(cub octahedral) site. The corresponding ionic radii of Ba^{2+} (12 coordinate ionic radius, 1.61 Å and 6 coordinate ionic radius. 1.35 Å) [25]; Sr^{2+} (1.44 and 1.18 Å), Ta^{5+} (0.64 Å) [25] cations suggest that the (Ta^{5+}) and one Sr^{2+} cation will occupy the 6-coordinate sites whereas the Ba^{2+} or a mixture of Sr^{2+} and Ba^{2+} will occupy the cub octahedral sites.

The Rietveld refinements, using synchrotron X-ray powder diffraction data, confirmed the ordering of the two *B*- site cations and established the distribution of these. Refinement of the structure of $BaSr_2TaO_{5.5}$ (acetone), assuming Sr only occupies the octahedral sites gave R_p = 3.21 % and R_{wp} = 4.77 %. The fractional positions were *A* ($\frac{1}{4}$, $\frac{1}{4}$, $\frac{1}{4}$), *B** (0, 0, 0), *B* ($\frac{1}{2}$, $\frac{1}{2}$, $\frac{1}{2}$) and O (x, 0, 0) with $x \sim 0.25$. Refinements where the Sr and Ta were allowed to disorder over the two appropriate sites (anti-site disorder) did not significantly alter the quality of the fits R_p = 3.15 % and R_{wp} = 4.63 % and indicated less than 3 % of the Ba was mixed in the octahedral site. Figure 2 illustrates the Rietveld refinement profiles for the ordered model of $BaSr_2TaO_{5.5}$. The pattern contains a number of weak and somewhat broadened reflections that are more pronounced at low angles originating from traces of a second perovskite phase. Consequently, a two-phase model was utilized where the major phase was in $Fm\bar{3}m$ and the minor phase in $Pm\bar{3}m$ where the cations were disordered over the two sites appropriate to the stoichiometry. The oxides obtained using water during the mixing were found to have similar atom distributions to those made by using acetone suggesting that, as expected, the reaction media had a little impact on ordering. Table 6.1 presents the results of the structure refinement of the $BaSr_2TaO_{5.5}$.

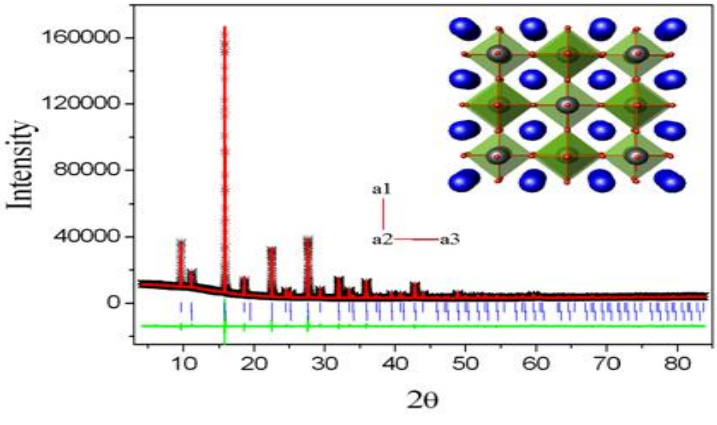

Figure 2: Synchrotron X-ray diffraction profiles for $BaSr_2TaO_{5.5}$ (acetone). The data are represented by the crosses and the solid lines are the calculated

and difference profiles. The positions of the space group allowed reflections are shown by the vertical markers immediately below the observed profile. Upper marks are from the major phase and lower marks for the minor $Pm\bar{3}m$ phase. A representation of the ordered $BaSr_2TaO_{5.5}$ structure is also included.

Table 1: Structural parameters for $BaSr_2TaO_{5.5}$ as obtained from the Rietveld refinement against powder synchrotron diffraction data.

Atom	*site*	*x*	*y*	*z*	B_{iso} ($Å^2$)	*Occupancy*
Major Phase		$Fm\bar{3}m$	a = 8.4539(6) Å			Z = 8
Ba/ Sr	8(*c*)	0.25	0.25	0.25	3.97(3)	0.5/0.5
Sr	4(*a*)	0	0	0	4.90(5)	1
Ta	4(*b*)	0.5	0.5	0.5	0.30(1)	1
O	24(*e*)	0.2741(5)	0	0	5.74(2)	0.92(2)
Manor Phase		$Pm\bar{3}m$	a = 4.2154(1) Å			Z = 1
Ba	1(*b*)	0.5	0.5	0.5	0.33(16)	1
Ta	1(*a*)	0	0	0	0.10(11)	1
O	3(*b*)	0.5	0	0	7.53(15)	0.71(3)
R- factor		R_p = 3.15 %, R_{wp} = 4.63 %, χ^2 = 8.93.				

Table 2 provides the values of lattice parameters, unit cell volumes and *x* coordinate of the oxygen for the different compositions. The cell volumes are slightly higher where water was employed in the reaction than in the acetone treated samples. This result corresponds to the effect of water on the oxides texture where the grain sizes and the cell volumes increase by adding water to the initial

reaction. It is thought that in these samples the absorbed water interacted with the framework oxygen resulting in small displacements of the atoms.

Table 2: Lattice parameters (*a*), unit cell volumes (V) and *x* coordinate of the oxygen for different compositions of $BaSr_2TaO_{5.5}$ as obtained from the Rietveld refinement against powder synchrotron diffraction data.

Formula	*a* (Å)	V ($Å^3$)	*x*
$BaSr_2TaO_{5.5}$ (acetone)	8.4539(6)	604.186(1)	0.2729(6)
$BaSr_2TaO_{5.5}$ (water)	8.4803(4)	609.955(6)	0. 2708(5)

Since the refinement using the XRD data did not locate the light oxygen atoms with certainty, neutron diffraction was employed to better describe the position of oxygen atoms and to aid in the refinement of any non-stoichiometry. Neutron diffraction data were collected for the $BaSr_2TaO_{5.5}$ (water). Compared to other oxides studied this oxide, displayed a significant difference in the cell volume between the two synthetic methods. A striking feature of the neutron diffraction profiles for $BaSr_2TaO_{5.5}$ s the presence of diffuse intensity in the form of a modulated background (Figure 3). Since there is only one anion site in the ideal structure it is not possible to have an ordered arrangement of the anion vacancies. The diffuse structure was not apparent in the X-rays profiles suggesting that the modulated background is associated with disorder of the lighter atoms. The disordered phase evident in the synchrotron profiles of $BaSr_2TaO_{5.5}$ was not observed in the corresponding neutron profile, presumably as a result of the lower peak with resolution of the neutron profiles.

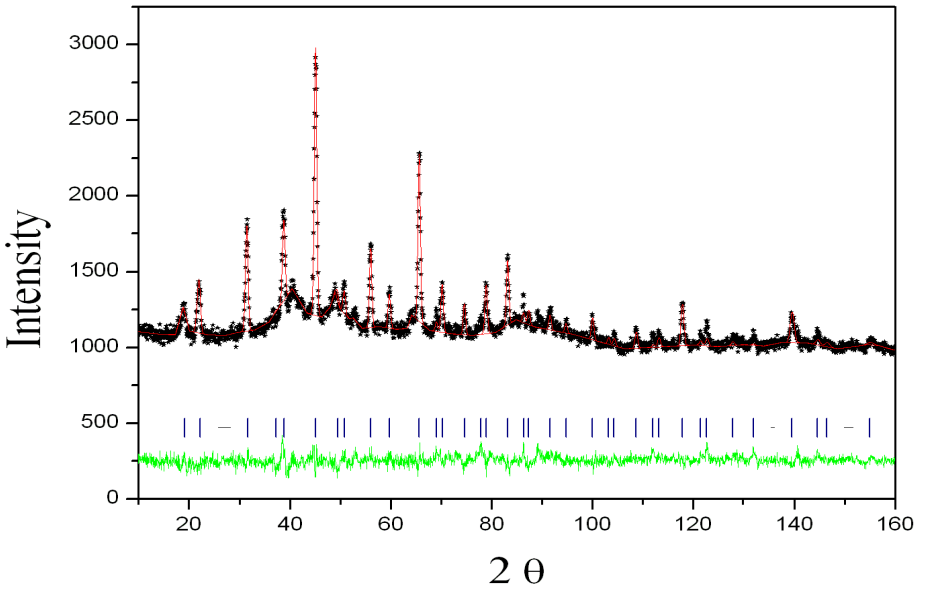

Figure 3: Neutron diffraction profiles for $BaSr_2TaO_{5.5}$ (water). The data are represented by the crosses and the solid lines are the calculated and difference profiles. The positions of the space group allowed reflections are shown by the vertical markers immediately below the observed profile.

Accordingly, the refinements of the structure of $BaSr_2TaO_{5.5}$ against the neutron diffraction data were performed using the same model suggested by Zhou *et al.* [15] where the Ba(1), Sr (1) and oxygen were disordered at the cuboctahedral and anion sites respectively. As found by Zhou *et al*., the refinements showed evidence for *A* cation and anion displacive disorder in the two oxides structures.

Table 3: Results of the structural refinements for $BaSr_2TaO_{5.5}$ (water) using neutron powder diffraction data.

	Atom	*x*	*y*	*Z*	B_{iso} ($Å^2$)	*Occ*
$BaSr_2TaO_{5.5}$	Ba/Sr(1)	0.2736(8)	0.2736(8)	0.2736(8)	3.20(29)	1
	Sr(2)	0	0.033(2)	-0.033(2)	1.76(74)	0.77(1)
	Ta	0.5	0.5	0.5	1.97(08)	1
	O(1)	0.2708(5)	0	0	3.90(10)	0.67(1)

	O(2)	0	0.169(1)	0.169(1)	3.88(54)	0.09(1)
	R- factors	R_p = 3.41 %, R_{wp} = 4.46 %, χ^2 = 1.45				

As summarised in table 3, a $\langle 01\bar{1} \rangle$ displacement of the 4*a* cation at (0, 0, 0) onto a 48*i* site at (0, *y*, -*y*) with $y \sim 0$ was evident and such displacement gave an optimal fit to the neutron data. The occupancy of the 48*i* site was refined and gave the required stoichiometry. Examination of the Fourier maps generated by Rietica revealed the presence of nuclear density near 0 1/6 1/6, corresponding to a 48*h* site in $Fm\bar{3}m$. The Fourier transform is a useful probe in the crystallography since the difference map can be used to locate missing atoms in a crystal structure [33]. The Fourier difference maps provided evidence for the presence of the protons (water) in the structure as suggested by TGA analysis. The measured neutron and synchrotron X-ray diffraction profiles show no evidence for superlattice peaks associated with tilts.

Thermal analysis

Thermal analysis measurements (TGA and VT-XRD) demonstrate a weight loss and an unusual thermal expansion upon heating for the oxides prepared using water during the mixing. Figure 4 shows the thermal decomposition curve of $BaSr_2TaO_{5.5}.nH_2O$ in the temperature range 30-600 °C and under a nitrogen atmosphere. These measurements were performed immediately after sample preparation. The initial weight loss for both samples at temperatures of $\leq$ 100 °C is believed to be due to the loss of chemisorbed water. That this occurs below 100 °C reflects the use of a dry N_2 atmosphere in the measurements. The observed weight loss near 550 °C is indicative of the removal of the water molecules that occupied the nominally vacant anion sites. At higher temperature, the sample weight is essentially constant demonstrating that all the water is lost from the lattice by ~ 600 °C.

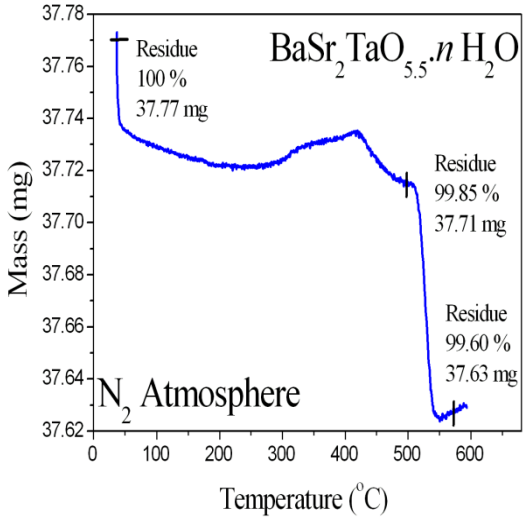

Figure 4: Thermogravimetic curves for $BaSr_2TaO_{5.5}.nH_2O$ under a nitrogen atmosphere.

From the TGA measurements, *n* in $BaSr_2TaO_{5.5}.nH_2O$ were found to be 0.10 moles per formula unit respectively. The inclusion of water in the oxides suggests the possibility of proton conduction, which might be lost at high temperatures as consequence of the loss of water.

Variable temperatures XRD (VT-XRD) data reveals a possible mechanism of the water interaction with the material. As shown in figure 5, initial heating results in normal thermal expansion of the unit cell volumes of $BaSr_2TaO_{5.5}.nH_2O$ in which both the *A*-O and *B*-O distances increase. Between 250 and 350 ºC, the cell volumes decreases as a result of water loss. Above 350 ºC, the heating, again, results in normal thermal expansion suggesting total removal of the lattice water. The importance of water is reflected in linear thermal contraction upon cooling. A similar observation has been reported for the $Sr_2MSbO_{5.5}$ (M = Ca^{2+}, Sr^{2+} and Ba^{2+}) system [15]. In this earlier work it was stated that a combination of local clustering of the anions and vacancies together with water–water and water–host hydrogen bonds plays a role in defining the volume of the encapsulated water clusters and that changes in the local structure upon heating result in the anomalous thermal expansion observed in variable temperature diffraction measurements [15]. In that work, the temperature at which the cell size begins to decrease upon heating was

found to be dependent on the size of the cation and increases in the order Ca < Sr < Ba [15]. The movement of the oxygen into the interstitial sites is thought to be also important since this is coupled with large displacements of the *A*- and *B*-site cations and gives a broad distribution in bond lengths [16].

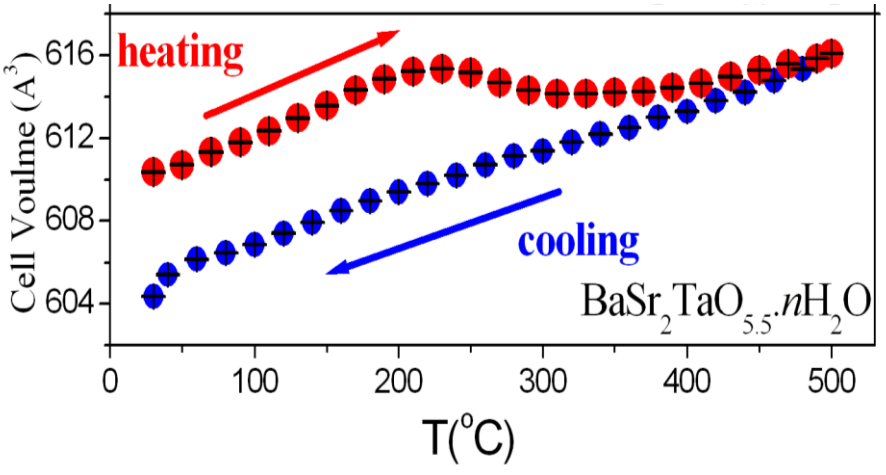

Figure 5: Temperature dependence of the cell volume for $BaSr_2TaO_{5.5}.nH_2O$. The red circles are the results obtained during the heating cycle and the blue circles those during cooling. The sample vacuum was 1×10^{-3} Torr during the measurements.

Conclusion:

The impact of changing the conditions used to prepare $BaSr(SrTa)O_{5.5}$ was investigated. The oxide was prepared using acetone and aqueous solvents as media of the reactions. The two synthetic methods produce monophasic powders that differ in color, particle size, and hardness. It is found that mixing water with reactants influences the morphology and the texture of the oxides resulting in yellowish color, larger grain size and rougher surfaces. The oxide form a cation ordered double perovskite structure and have a $Fm\bar{3}m$ cubic lattice arrangement. There is no evidence for cation mixing between the *A* and *B* sites. The compound obtained by reaction with water has larger cell volumes than those obtained by reaction with acetone. This suggests a role of hydrogen bondings of water with the oxygen lattice. The neutron diffraction profiles for $BaSr_2TaO_{5.5}$ (water) showed the presence of diffuse structure as a consequence of disorder of oxygen atoms. The structural refinements provide evidences for anion deficiency and a displacive disorder of *A* cations into the structures. The oxides demonstrate a weight loss

upon heating due to the presence of water within the structures. The observation of unusual thermal expansion of the unit cells is explained by the presence of water and vacancies in the structure. It is believed that the movement of the oxygen into the interstitial sites results in large displacements of the *A*- and *B*-site cations and broad bond length distribution. There is the possibility of proton conduction which would be reduced at elevated temperatures as consequence of the loss of water.

References

[1] K.W. Browall, O. Muller, R.H. Doremus, *Materials Research Bulletin*, 11 (1976) 1475-1481.

[2] N.L. Ross, R.J. Angel, L.W. Finger, R.M. Hazen, C.T. Prewitt, *Journal of American Chemical Society*, 351 (1987) 164-172.

[3] J. Lecomte, J.P. Loup, M. Hervieu, B. Raveau, *Physica Status Solidi*, 65 (1981) 743-752.

[4] A.S. Nowick, Y. Du, *Solid State Ionics*, 77 (1995) 137-146.

[5] R. Glöckner, A. Neiman, Y. Larring, T. Norby, *Solid State Ionics*, 125 (1999) 369-376.

[6] I. Animitsa, A. Neiman, A. Sharafutdinov, S. Nochrin, *Solid State Ionics*, 136–137 (2000) 265-271.

[7] I. Levin, J.Y. Chan, R.G. Geyer, J.E. Maslar, T.A. Vanderah, *Journal of Solid State Chemistry*, 156 (2001) 122-134.

[8] I. Levin, L.A. Bendersky, J.P. Cline, R.S. Roth, T.A. Vanderah, *Journal of Solid State Chemistry*, 150 (2000) 43-61.

[9] E.L. Colla, I.M. Reaney, N. Setter, *Journal of Applied Physics*, 74 (1993) 3414-3425.

[10] C.J. Howard, B.J. Kennedy, P.M. Woodward, *Acta Crystallographica Section B*, 59 (2003) 463-471.

[11] Q. Zhou, B.J. Kennedy, M. Avdeev, *Journal of Solid State Chemistry*, 183 (2010) 1741-1746.

[12] G. King, P.M. Woodward, *Journal of Materials Chemistry*, 20 (2010) 5785-5796.

[13] T. Norby, *Journal of Materials Chemistry*, 11 (2001) 11-18.

[14] I. Animitsa, T. Norby, S. Marion, R. Glöckner, A. Neiman, *Solid State Ionics*, 145 (2001) 357-364.

[15] Q. Zhou, B.J. Kennedy, M. Avdeev, *Journal of Solid State Chemistry*, 184 (2011) 2559-2565.

[16] G. King, K.J. Thomas, A. Llobet, *Inorganic Chemistry*, 51 (2012) 13060-13068.

[17] K.S. Wallwork, B.J. Kennedy, D.A. Wang, *AIP Conference Proceedings*, 879 (2007) 879-882.

[18] B.A. Hunter, C.J. Howard, RIETICA. A Computer Program for Rietveld Analysis of X-Ray and Neutron Powder Diffraction Patterns, (1998)

[19] K. Liss, B. Hunter, M. Hagen, T. Noakes, S. Kennedy, *Physica B*, 385–386 (2006) 1010–1012.

[20] I. Animitsa, A. Nieman, S. Titova, N. Kochetova, E. Isaeva, A. Sharafutdinov, N. Timofeeva, P. Colomban, *Solid State Ionics*, 156 (2003) 95-102.

[21] V.M. Goldschmidt, *Naturwissenschaften*, 14 (1926) 477-485.

[22] L. Chai, P.K. Davies, *Journal of the American Ceramic Society*, 80 (1997) 3193-3198.

[23] W. Dmowski, M.K. Akbas, T. Egami, P.K. Davies, *Journal of Physics and Chemistry of Solids*, 63 (2002) 15-22.

[24] Q. Zhou, B.J. Kennedy, J.A. Kimpton, *Journal of Solid State Chemistry*, 184 (2011) 729-734.

[25] R.D. Shannon, *Acta Crystallographica Section B*, 26 (1970) 447-449.

[26] I. Animitsa, T. Denisova, A. Neiman, A. Nepryahin, N. Kochetova, N. Zhuravlev, P. Colomban, *Solid State Ionics*, 162–163 (2003) 73-81.

[27] F. Galasso, L. Katz, R. Ward, *Journal of the American Chemical Society*, 81 (1959) 820-823.

[28] M. Murakami, K. Hirose, H. Yurimoto, S. Nakashima, N. Takafuji, *Science*, 295 (2002) 1885-1887.

[29] M. Alfredsson, J.P. Brodholt, D.P. Dobson, A.R. Oganov, C.R.A. Catlow, S.C. Parker, G.D. Price, *Physics and Chemistry of Mineral*, 31 (2005) 671-682.

[30] A. Shatskiy, H. Fukui, T. Matsuzaki, K. Shinoda, A. Yoneda, D. Yamazaki, E. Ito, T. Katsura, *American Mineralogist*, 92 1744-1749.

[31] A. Yeganeh-Haeri, D.J. Weidner, E. Ito, *Science*, 243 (1989) 787-789.

[32] S.D. Jacobsen, Z. Liu, T.B. Ballaran, E.F. Littlefield, L. Ehm, R.J. Hemley, *Physics of the Earth and Planetary Interiors*, 183 (2010) 234-244.

[33] E.J. Mittemeijer, P. Scardi, Diffraction Analysis of the Microstructure of Materials, 2004, Springer, New York.

[34] I. Levin, J.Y. Chan, J.H. Scott, L. Farber, T.A. Vanderah, J.E. Maslar, *Journal of Solid State Chemistry*, 166 (2002) 24-41.

[35] E. Chinarro, G.C. Mather, A. Caballero, M. Saidi, E. Morán, *Solid State Sciences*, 10 (2008) 645-650.

[36] W. Dmowski, K.E. Swider-Lyons, *Crystalline Materials*, 219 (2004) 136-142.

